Journal of Non-Crystalline Solids 495 (2018) 54–58

Contents lists available at ScienceDirect

Journal of Non-Crystalline Solids

journal homepage: www.elsevier.com/locate/jnoncrysol

Stress effects on magnetic property of Fe-based metallic glasses

M.C. Ri[a,c], D.W. Ding[a,*], B.A. Sun[a], J.Q. Wang[b], X.S. Zhu[a], B.B. Wang[a], T.L. Wang[c,d], Q.Q. Qiu[d], L.S. Huo[e], W.H. Wang[a,*]

[a] Institute of Physics, Chinese Academy of Sciences, Beijing 100190, P.O. Box 603, China
[b] Ningbo Institute of Materials Technology and Engineering, Chinese Academy of Sciences, Ningbo, Zhejiang 315201, China
[c] University of Chinese Academy of Sciences, Beijing 100049, China
[d] Institute of Electrical Engineering, Chinese Academy of Sciences, Beijing 100190, China
[e] Ningbo Zhongke B Plus New Materials Technology Co., Ltd., Ningbo 315201, China

ARTICLE INFO

Keywords:
Soft magnetic materials
Bending stress
Stress relief
Structural relaxation

ABSTRACT

The investigation on the stress relief of magnetic materials is important both for the industrial process and the academic research. In this work, the stress effects on the magnetic characteristics in Fe-based metallic glasses (MGs) are investigated under the applied bending stress and various annealing treatments. It was found that both the magnetic induction intensity $\boldsymbol{B}$ and effective permeability $\boldsymbol{\mu'}$ decrease while coercivity $\boldsymbol{H_c}$ increases with the applied compressive stress, indicating that the compressive effect is dominant on the magnetic characteristics in $Fe_{78}Si_9B_{13}$ MG ribbons. We also found that the wide domain wall movement and the rotation of the narrow domains are seriously affected by internal stress during the magnetization process. Our results reveal that the stress relief plays a critical role in improving magnetic properties of Fe-based MGs and are helpful for understanding the correlations between the stress, microstructure change and magnetic softness in magnetic MGs.

1. Introduction

Ferromagnetic metallic glasses (MGs) can be widely used in various electronic devices such as transformers, reactors, motors and mutual inductors. Ferromagnetic MGs with higher saturated magnetic flux density ($\boldsymbol{B_s}$), lower coercivity ($\boldsymbol{H_c}$), higher permeability ($\boldsymbol{\mu}$), better mechanical properties and lower materials cost [1–4], are promising candidates to replace traditional soft magnetic crystalline materials, and therefore attracted considerable research interests over past decades. In general, the amorphous alloys obtained by rapid quenching from the melt are often in a metastable nature. As a result, their microstructure and properties can easily be changed by subsequent heat treatment or mechanical deformation [5,6]. The magnetic MGs lack the magentocrystalline anisotropy as usually found in crystalline alloys. However, due to the internal stress developed along the ribbon axis during melt-quenching process and the interaction between elastic stress and spontaneous magnetization, their magnetic properties are also sensitive to the external stress and the thermal history [7,8]. Supplementary treatments were often introduced for removing the internal stress [9–11]. For example, it has been reported that desirable soft magnetic properties in MGs can be achieved by many stress-relieving techniques, such as conventional annealing below Curie temperature [5,6], flash annealing [9,12,13] and cryogenic thermal cycling (CTC) after conventional annealing [3].

However, even after annealing, there are still many factors that can cause the internal stress in the magnetic MG materials. As a result, extensive experimental and theoretical investigations have been dedicated to the relationship between the internal stress and magnetic parameters such as magnetic domain [14–16], magnetization process [17,18], magnetic saturation [19,20], coercively [21,22], effective permeability [20,21], etc. in magnetic MGs of various forms, like wires [19,23], thin films [24,25], ribbons [26,27] and bulk samples [28–31]. Despite of these efforts, there are still a lot of inconsistency in the experimental results and discrepancies in the theoretical analysis among these many kinds of magnetic MGs. Particularly, a quantitative understanding on the contribution of stress to the magnetization process and the influence of stress relief on the magnetic properties in MGs during the post-processing [32] are not yet clear.

In this work, we investigated the magnetization process of disk-shaped Fe-based samples. The effects of structural relaxation on internal intrinsic stress relief and the effect from subsequent external applied stresses on the magnetic properties are systemically studied. These results are helpful for designing stress-sensitive components.

* Corresponding authors.
E-mail addresses: dingdawei@iphy.ac.cn (D.W. Ding), whw@iphy.ac.cn (W.H. Wang).

https://doi.org/10.1016/j.jnoncrysol.2018.05.017
Received 5 January 2018; Received in revised form 8 May 2018; Accepted 9 May 2018
Available online 14 May 2018

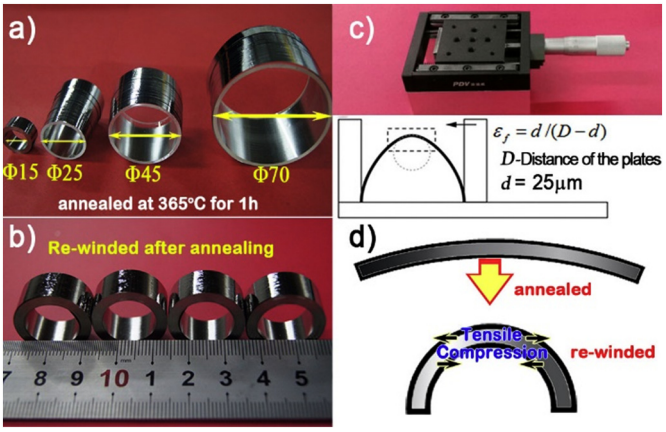

Fig. 1. (a) The mandrel-winded samples with the different radius of curvature after annealing under 365 °C for 1 h time, (b) the re-winded samples with the same internal diameter of 15 mm, (c) the relative strain at fracture (RSF) equipment and experimental method, (d) schematic diagram of magnified region of the ribbon indicating the stress state. During re-winding the bending process causes the external layered stresses-tensile near the surface on the free side and compressive underneath on the wheel side.

2. Experiments

The MG ribbons of $Fe_{78}Si_9B_{13}$ (supplied by An Tai Inc. of *China Iron & Steel Group*) with a uniform thickness of 25 μm and a width of 10 mm were prepared by the melt-spun technique. The amorphous nature of as-cast and annealed specimens was ascertained by X-ray diffraction (XRD, Bruker D8 Advance) with CuK_α radiation and differential scanning calorimetry (DSC, Perkin Elmer DSC8000). The anelastic structural relaxation behavior was explored using DSC [33–35] after annealing for 10 min, 1, 2, 3 h at $T = 365$ °C in a purified argon atmosphere at a heating rate of 20 K/min. The values of density ρ were obtained by the Archimedean technique.

For evaluation of subsequent stress effects after structural relaxation, the MG ribbons were mandrel-winded with various radius of curvature $r_{a,i}$ (*i*-indexed sample's radius) [initial internal diameter $\Phi_{in} = 2r_{a,i} = 15$, 25, 45, 70 mm, ∞(straight sample)] and then annealed at 365 °C for 1 h (Fig. 1a). All metallic glass ribbons for measurements of magnetic properties have the same length of 7 m. The $Fe_{78}Si_9B_{13}$ ribbons maintain the curvature after annealing because the stress is released completely during the annealing process [36]. In order to evaluate the embrittlement of the ribbons due to the annealing of winded samples on mandrels of different radii, the relative strain at fracture (RSF), which was represented by $\varepsilon_f = d/(D-d)$ (D is the distance between two parallel plate, d is the ribbon thickness) [37,38] was measured (Fig. 1c).

The samples were removed from the mandrel after annealing, then re-winded to a smaller curvature diameter of $\Phi_{in} = 2r_s = 15$ mm, as shown in Fig. 1b. After being curved into a smaller curvature, stresses were introduced again (tension in outer surface and compression in inner surface), as shown in Fig. 1d. The stress was greater for the cores with a larger initial curvature radius.

The magnetic induction and coercivity were measured using a *B-H* loop tracer (MATS 2010SD) under a maximum applied field of 800 A/m. The exciting and searching coils are 20 turns and 2 turns. The effective permeability at various frequency (0.1, 1, 10, 100 kHz) was measured by using an impedance analyzer (Agilent 4294A) equipped with a test fixture (16047E). The inductance of the samples was measured to characterize the magnetic effective permeability. When the ferromagnetic sample is magnetized by an AC excitation magnetic field, the magnetic effective permeability is expressed as a following form, $\mu' = L_s/L_0 = L_s 2\pi/\left(\mu_0 N^2 h \ln\left(\frac{or}{ir}\right)\right)$, where L_s & L_0 are effective inductance (H) of the core with winding and inductance of the coil. N is the number of turns of the coils, h is the height of the toroidal core (mm). *or* & *ir* are the outer and the inner diameter of the toroidal core (mm), μ_0 is the permeability of the vacuum: $4\pi \times 10^{-7}$ [39–41]. To avoid accidental error, every measurement was performed over 3 samples and every data point was the average of 3 to 5 observations, especially 100 times for RSF measurement.

3. Results and discussions

The DSC results show that the value of T_c increases obviously with the annealing temperature and time, indicating that the isothermal annealing induces the structural relaxation due to the free volume reduction [33,42] and the annealing treatment affects the electron energy state of the MGs. Following the mean field theory, T_c depends on the exchange integral [43]. In the molecular field approximation, Curie temperature is expressed as

$$T_c = \frac{2S(S+1)}{3k} \sum_{ij} J_{ij} \tag{1}$$

where S is atomic spin, k is the Boltzmann constant, and J_{ij} represents the exchange interaction between atoms i and j [44,45]. It implies that isothermal annealing induces the change of the exchange integral.

The attempt to eliminate the pure external stress effect by making samples out of toroidal shapes with various radius of curvature was performed (Fig. 1). As shown in Fig. 2a, the RSF value decreases with the increase of the mandrel-winded radius, which can be well-fitted by a power law. This suggests that a plastic deformation have been occurred after annealing. After re-winding, the internal stress increases logarithmically according to the magnitude of the mandrel-winded radius (see the inset of Fig. 2b). During re-winding, the bending can cause external layered stresses that are tensile near the outer surface and compressive near the inner [46]. Fig. 2 (b) shows the variations of induced strain and the internal stress with the radius of the mandrel-

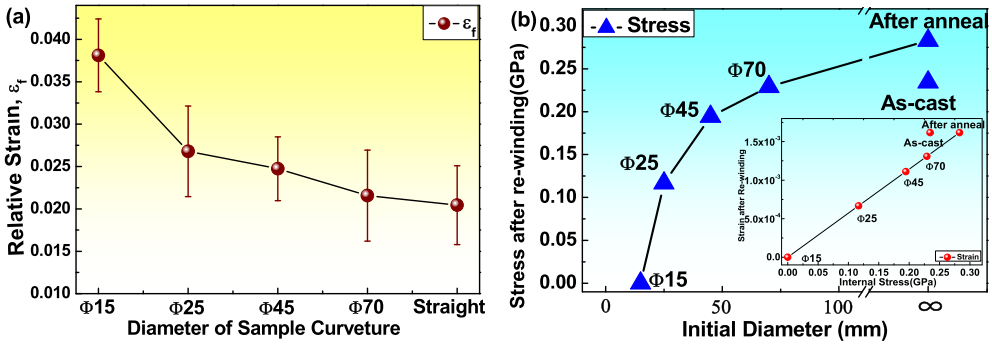

Fig. 2. (a) The relative strain at fracture on the bended samples with the different radius of curvature after annealing; (b) The relationship between partial internal stress and initial diameter which implies the logarithmic increase of stress to the initial diameter. The insert shows the induced partial strain of the samples after re-winding and partial internal stress in the minimum radius layer part of the mandrel-winded samples. Because of the different elastic moduli for the straight samples [48] the partial stress of as-cast samples is smaller than of the annealed samples. The values of the Young's moduli were refer-

enced for as-cast ($E_{as}(H = 800A/m) \approx 145$ GPa) and annealed samples ($E_{t_{an}} = 350(H = 800A/m) \approx 175$ GPa) [47].

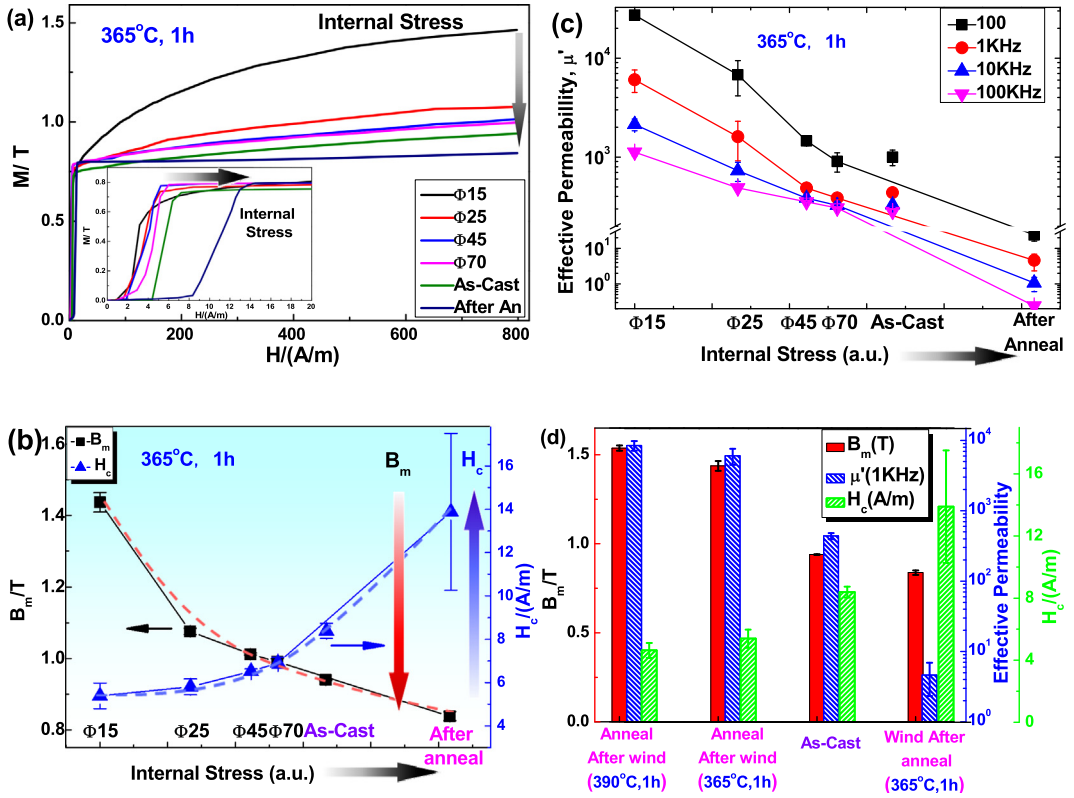

Fig. 3. (a) The magnetization curve, (b) magnetic induction and coercivity and (c) effective permeability changes of the re-winding samples (Fig. 1) as a function of internal stress. The magnetization gradient of all the samples reaches the maximum value near 0.5–0.75 T in magnetization curves. The inset of (a) shows that in accordance with growth of internal stress the irreversible movement region of the wide domain wall moves to the higher magnetic field. (d) the magnetic property changes by internal stress relief.

winded samples, respectively. According to Hooke's law, the stress for continuous media is proportional to strain. The homogenous elastic strain ε induced by winding can be estimated as$\varepsilon = d/2r$, where d is the thickness of ribbon and r is the minimum curvature radius of released ribbon [46]. Therefore, the applied bending stresses after re-winding were proportional to the difference between the inverse number of radius curvature values, i.e. $1/2r_s - 1/2r_{a,\,i}$ ($r_s \le r_{a,\,i}$, where $r_{a,i}$ is the initial radius and r_s is the final sample's radius). When the values of $r_{a,i}$ & r_s are equal, there is no internal stress by applied deformation in MGs in principle, even though it cannot completely remove the internal stress due to the rapid quenching manufacture process. For as-cast and annealed straight samples, the value of $r_{a,i}$ can be regarded as infinitely large. So the value of relative strain for the re-winded as-cast sample (marked in the figure as “As-cast”) and annealed samples (marked in the figure as “After anneal”) should be the same, yet their stress values are quite different due to the difference of elastic moduli between as-cast and annealed samples [47,48]. As a result, the partial internal stress for as-cast samples is smaller than that for the annealed.

The changes of magnetic property as a function of applied external stress (or internal stress) are shown in Fig. 3. The common feature is that the magnetization curves of all samples have the maximum gradient near the magnetization of 0.5–0.75 T, and then their slopes become gentle (Fig. 3a). Compared to the normal magnetization process [11], the wide domain wall movement region was broadened (Fig. 3a inset) and subsequently the maximum slope in the magnetization curve become gentle due to the internal stress. This extended wide domain wall movement regions could affect the magnetic coercivity and the slope of magnetization curve after the maximum-gradient. Within the framework of the statistical pinning potential model, it is clear that once the magnetization passed through the irreversible rotational process, the magnetization could no longer decrease with the increasing field. As a result, there is a suppressible limit for magnetic induction, where the magnetization process of magnetic MGs can no longer decrease with increasing field even the stress increases more largely (Fig. 3a). When increasing the internal stress by applied external deformation, the magnetic induction shows a non-linear decrease with the non-linear growth of the coercivity (Fig. 3b).

It is noted that that the magnetic properties of the annealed samples are poorer than the as-cast samples, indicating that internal stress of annealed samples is greater than those as-cast. After applying the external deformation, the magnetic induction was reduced by as much as 58.3% (from 1.44 T to 0.84 T) and the coercivity was increased by 257.8% (from 5.38 A/m to 13.89 A/m). The variations of magnetic induction (52.9% increment from 0.94 T for as cast to 1.44 T for annealed) and coercivity (−35.8% decrement from 8.39 A/m for as cast to 5.39 A/m for annealed) of the samples with the diameter of $\Phi_{in} = 2r_s = 15$ mm can be attributed to the overlap effects of both the internal intrinsic and external applied stress relief, which are induced by the quenching process and by the bending process, respectively.

The measurements on sample density show that the density grows by 0.3% after annealing for 3 h at 365 °C as compared to as-cast samples. By combining the results from DSC, it can be regarded that the change of T_c reflects the change of exchange integral and the atomic density in MGs. From the relationship between saturation magnetization and Curie temperature $M_s = M(0)(1 - T/T_c)^{0.36}$ [49–51], we can reasonably assumed that the change of magnetic induction is a reflection of the atomic density. Based on these facts, one can infer that the change of magnetic induction is related to not only the stress relief, but also the density change even though the latter effect is small. Fig. 3(c) shows that the variation of magnetic effective permeability with the internal stress. From the plot, one can see that the effective permeability is also reduced with increasing internal stress, indicating an

effect of the stress relief on the magnetic effective permeability. From these phenomena, a quantitative relationship between the stress relief effect and magnetic properties including magnetic induction, coercivity and effective permeability in Fe-based MGs can be constructed. To illustrate the stress relief effect on magnetic properties due to both internal stress as induced by applied deformation and by the quenching process, the experimental result for the annealed at 390 °C–1 h samples after winding as Φ_{in} = 15 mm was also shown in Fig. 3(d). Clearly, samples annealed for 390 °C–1 h show the better soft magnetic properties.

From the results above, we found large changes in all magnetic properties including magnetic induction, coercivity and effective permeability under the applied magnetoelastic stress. This may be originated from the pinning effect as related to the magnetoelastic stress induced by bending deformation. Under the stress of both bending deformation and the quenching process, the MG samples have high potential energy. In the lower magnetic field, this potential energy could shift the irreversible rotation region of the wide domain to the higher field, yielding the increase of magnetic coercivity and the decrease of the effective permeability with internal stress. In the higher external applied magnetic field, the magnetic polarization could overcome this imposed stress energy as well as spontaneous magnetization energy intrinsic to the material.

The stress effect on the magnetic characteristics can be discussed using the framework J-A (Jiles-Atherton) model, due to the random magnetic anisotropy in the magnetic MGs. By applying the stress, the effective magnetic field by the magnetoelastic energy is defined as [20].

$$H_\sigma = \frac{3}{2}\frac{\sigma}{\mu_0}\frac{\partial\lambda}{\partial M}(\cos^2\varphi - \nu\sin^2\varphi) \tag{2}$$

where λ is the magnetostriction constant, σ is the stress, ν is the Poisson's constant, ϕ is the angle between the magnetization and the stress axis μ_0 is the permeability of the vacuum. Following the extended J-A model [20,28], the change of magnetization M with the applied field can be taken as

$$\frac{dM}{dH} = \frac{1}{\delta k/\mu_0 - \alpha(M_{an} - M)}(M_{an} - M) \tag{3}$$

where α is an experimentally determined mean field parameter representing interdomain coupling, M_{an} is the anhysteretic magnetization, k is the pinning coefficient. Many ferromagnetic materials, including amorphous and nanocomposite magnets, exhibit an induced roll anisotropy when they are processed in a magnetic field [20,52]. It is considered that the stress is along the direction of applied field (Fig. 1), so the angle θ between applied field and stress axis is equal to zero. In this case the changes of magnetic characteristics with respect to stress (Fig. 3b, c) are quite similar to the case of compressive stress for $\theta = 0$ in the former work [20,21]. It could be regarded that the compressive stress effect to the magnetic characteristics is dominant for present work.

The change behavior of the magnetization curve with respect to stress should have an origin of the domain structure as well as of the microstructure. Based on the statistical pinning potential model [11], the unique behavior observed here such as the change of the magnetization process (Fig. 3a), increase of coercivity & decrease of magnetic induction by applied compressive stress (Fig. 3b) can be attributed to the domain wall movement and rotation [18,22]. First, the large variation in the magnetic induction with compressive stress is due to the increase of magnetoelastic coupling as a result of the irreversible rotation of narrow domains in the magnetization curve. There is a suppressible limit for magnetic induction in the magnetization process of magnetic MGs, which cannot be further reduced for large stress. Second, the large variation in magnetic coercivity and effective permeability by compressive stress in MGs should arise from the domain wall movements. Therefore, removing the compressive stress in the region of domain wall movement and rotation could be an efficient method to improve softness in Fe-based amorphous ribbons.

4. Conclusion

To summarized, we report large changes in magnetic properties of Fe-based metallic glasses (MGs) such as magnetic induction ($\boldsymbol{B}$), coercivity ($\boldsymbol{H_c}$) and effective permeability ($\boldsymbol{\mu'}$) under applied magnetoelastic stress. By investigation of Curie temperature and density change under various annealing treatment, we found that denser atom's packing affect to the magnetic induction of Fe-based MGs. Based on the extended J-A model, we experimentally found that: 1) The compressive effect is dominant on the magnetic characteristics during the external applied stress in Fe-based amorphous ribbons; 2) The large variation in the magnetic induction by compressive stress is due to the irreversible rotation, but there is a suppressible limit for magnetic induction in the magnetization process of magnetic MGs after adding larger stress; 3) The large variation in magnetic coercivity and effective permeability by compressive stress in the MGs is due to the domain wall movements. The observation is helpful for understanding the correlations between the stress relief, microstructure change and magnetic softness in magnetic MGs as well as for improving the soft magnetic properties of metallic glassy materials.

Acknowledgements

This work was supported by National Key Research and Development Plan (Grant No. 2016YFB0300500, 2017YFB0903900), the Key Research Program of Frontier Sciences, CAS (Grant No. QYZDY-SSW-JSC017), the financial support of the NSF of China (Grant No. 51571209, 51461165101, 51601215, and 51301194) and the National 973 project (Grant No. 2015CB856800). We thank B. S. Dong and S. X. Zhou in An Tai Inc. of *China Iron & Steel Group* for supplying samples and Y. P. Xu and D. S. Shang in the Institute of Physics (CAS) and A. D. Wang in the Ningbo Institute of Materials Technology and Engineering (CAS) and J. H. Gye in the Department of Solid State Mechanics, University of Sciences of DPRK for experimental assistance and helpful discussion, CAS-TWAS support.

References

[1] B. Huang, Y. Yang, A.D. Wang, Q. Wang, C.T. Liu, Intermetallics 84 (2017) 74.
[2] A. Inoue, B.L. Shen, Mater. Trans. 43 (2002) 766.
[3] M.C. Ri, S. Sohrabi, D.W. Ding, B.S. Dong, S.X. Zhou, W.H. Wang, Chin. Phys. B. 26 (2017) 066101.
[4] F. Wang, A. Inoue, Y. Han, F.L. Kong, S.L. Zhu, E. Shalaan, F. Al-Marzouki, A. Obaid, J. Alloys Compd. 711 (2017) 132.
[5] T. Gheiratmand, H.R. Madaah Hosseini, P. Davami, M. Gjoka, G. Loizos, H. Aashuri, J. Alloys Compd. 582 (2014) 79.
[6] A. Hirata, N. Kawahara, Y. Hirotsu, A. Makino, Intermetallics 17 (2009) 186.
[7] F.E. Luborsky, Handbook of Ferromagnetic Materials, Elsevier, 1980, pp. 451–529.
[8] K. Mandal, M. Vázquez, D. Garcia, F.J. Castaño, C. Prados, A. Hernando, J. Magn. Magn. Mater. 220 (2000) 152.
[9] A.R. Yavari, R. Barrue, M. Harmelin, J.C. Perron, J. Magn. Magn. Mater. 69 (1987) 43.
[10] M.A. Escobar, A.R. Yavari, R. Barrue, J.C. Perron, IEEE Trans. Mag. 28 (1992) 1911.
[11] H. Kronmüller, Handbook of Magnetism and Advanced Magnetic Materials, vol. 2, John Wiley & Sons, Hoboken, 2007, pp. 677–1155.
[12] G. Herzer, V. Budinsky, C. Polak, Phys. Status Solidi B 248 (2011) 2382.
[13] Z.H. Sheng, J. Pang, X. Wang, K. Wen, L.Y. Guo, K.B. Kim, W.M. Wang, J. Non-Cryst. Sol. 448 (2016) 83.
[14] J.J. Becker, AIP Conf. Proc 29 (1976) 204.
[15] M. Tejedor, B. Hernando, J. Phys. D. Appl. Phys. 13 (1980) 1709.
[16] H. Alex, S. Rudolf, Magnetic Domains, Springer, Berlin Heidelberg, 2009, p. 696.
[17] A. Makino, C.T. Chang, T. Kubota, A. Inoue, J. Alloys Compd. 483 (2009) 616.
[18] L. Köszegi, H. Kronmüller, App. Phys. A 34 (1984) 95.
[19] A. Mitra, M. Vázquez, J. Magn. Magn. Mater. 87 (1990) 130.
[20] M.J. Sablik, S.W. Rubin, L.A. Riley, D.C. Jiles, D.A. Kaminski, S.B. Biner, J. Appl. Phys. 74 (1993) 480.
[21] D.C. Jiles, T.T. Chang, D.R. Hougen, R. Ranjan, J. Appl. Phys. 64 (1988) 3620.
[22] L. Callegaro, E. Puppin, Appl. Phys. Lett. 68 (1996) 1279.
[23] V. Zhukova, A. Zhukov, J.M. Blanco, J. Gonzalez, C. Gómez-Polo, M. Vázquez, J. Appl. Phys. 93 (2003) 7208.

[24] B. Zhu, C.C.H. Lo, S.J. Lee, D.C. Jiles, J. Appl. Phys. 89 (2001) 7009.
[25] D. Garcia, J.L. Munoz, G. Kurlyandskaya, M. Vazquez, M. Ali, M.R.J. Gibbs, IEEE Trans. Mag. 34 (1998) 1153.
[26] L. Kraus, P. Švec, J. Appl. Phys. 93 (2003) 7220.
[27] J.D. Livingston, Phys. Stat. Sol. (A) 56 (1979) 637.
[28] D.C. Jiles, D.L. Atherton, J. Magn. Magn. Mater. 61 (1986) 48.
[29] W. Fernengel, H. Kronmüller, J. Magn. Magn. Mater. 37 (1983) 167.
[30] H. Kronmüller, W. Fernengel, Phys. Stat. Sol. (A) 64 (1981) 593.
[31] H. Kronmüller, M. Fähnle, M. Domann, H. Grimm, R. Grimm, B. Gröger, J. Magn. Magn. Mater. 13 (1979) 53.
[32] D. Azuma, R. Hasegawa, S. Saito, M. Takahashi, J. Appl. Phys. 113 (2013) 17A339.
[33] J.S. Blázquez, S. Lozano-Pérez, A. Conde, Mater. Lett. 45 (2000) 246.
[34] S.G. Zaichenko, N.S. Perov, A.M. Glezer, E.A. Gan'shina, V.M. Kachalov, M. Calvo-Dalborg, U. Dalborg, J. Magn. Magn. Mater. 215 (2000) 297.
[35] Q. Hu, Z.H. Zhu, Rare Metal Mater. Eng. 44 (2015) 1340.
[36] X.F. Li, K. Zhang, C. Wang, W. Han, G. Wang, J. Mater. Sci. Technol. 23 (2007) 253.
[37] D. Maria, P.R. Ohodnicki, M.E. McHenry, M.A. Willard, Philos. Mag. 90 (2010) 1547.
[38] V.A. Fedorov, A.V. Yakovlev, A.N. Kapustin, Metal Science and Heat Treatment 50 (2008) 397.
[39] A.N. He, A.D. Wang, S.Q. Yue, C.L. Zhao, C.T. Chang, H. Men, X.M. Wang, R.W. Li, J. Magn. Magn. Mater. 408 (2016) 159.
[40] F. Kino, N. Chujo, K. Kume, T. Aoyama, M. Fukuda, J. Jpn. Soc. Powder Metallurgy 63 (2016) 618.
[41] Y.H. Ding, T. Qiu, X. Liu, Y. Long, Y.Q. Chang, R.C. Ye, J. Magn. Magn. Mater. 305 (2006) 332.
[42] M. Stoica, P. Ramasamy, I. Kaban, S. Scudino, M. Nicoara, G.B.M. Vaughan, J. Wright, R. Kumar, J. Eckert, Acta Mater. 95 (2015) 335.
[43] Y.X. Geng, Y.M. Wang, J.B. Qiang, G.F. Zhang, C. Dong, O. Tegus, J.Z. Sun, Intermetallics 67 (2015) 138.
[44] T.D. Shen, B.R. Sun, S.W. Xin, Intermetallics 65 (2015) 111.
[45] T. Mizoguchi, AIP Conf. Proc. 34 (1976) 286.
[46] Z. Lu, W. Jiao, W.H. Wang, H.Y. Bai, Phys. Rev. Lett. 113 (2014) 045501.
[47] Z. Kaczkowski, Applied Electromagnetics in Materials, Pergamon, Oxford, 1989, pp. 325–336.
[48] J.P. Yang, Q. Huang, D.G. Jiang, Hot Working Technology 37 (2008) 87.
[49] W.M. Yang, H.S. Liu, L. Xue, J.W. Li, C.C. Dun, J.H. Zhang, Y.C. Zhao, B.L. Shen, J. Magn. Magn. Mater. 335 (2013) 172.
[50] G. Herzer, IEEE Trans. Mag. 25 (1989) 3327.
[51] M. Stoica, V. Kolesar, J. Bednarčic, S. Roth, H. Franz, J. Eckert, J. Appl. Phys. 109 (2011) 054901.
[52] M.E. McHenry, D.E. Laughlin, Physical Metallurgy, Fifth Edition, Elsevier, 2014, pp. 1881–2008.